# Time-dependent non-linear buckling of 3D CFST arch structures with hybrid random interval uncertainties

Binhua Wu [a], Kang Gao [b, c]*, Jinpeng Feng [b], Gang Wu [b], Carol A. Featherston [c], Wei Gao [a], Weigang Zhao [d]**

[a] School of Civil and Environmental Engineering, The University of New South Wales, Sydney, NSW 2052, Australia

[b] School of Civil Engineering, Southeast University, Nanjing, China

[c] School of Engineering, Cardiff University, The Parade, Cardiff CF24 3AA, UK

[d] State Key Laboratory of Mechanical Behavior and System Safety of Traffic Engineering Structures, Shijiazhuang Tiedao University, Shijiazhuang 050043, China

## Abstract

Limit point and bifurcation buckling loads are critical concerns in structural stability design. With the inevitable viscoelastic effects of creep and shrinkage in concrete, such critical buckling points may vary due to the time-dependent change of equilibrium configuration. Furthermore, the intrinsic uncertainty and natural randomness in the geometry and material characteristics would affect the structural stability performance significantly. The present study provides a new robust method, called the generalized Chebyshev surrogate model-based sampling approach, in assessing the time-dependent nonlinear buckling behaviour of 3D concrete-filled steel tubular (CFST) arch structures when both random and interval uncertainties are involved. In the proposed approach, the relationships between the uncertain parameters and the critical nonlinear limit and bifurcation buckling loads are formulated using Chebyshev surrogate model strategy combined with finite element method. The extreme bounds of the statistical features, including means, standard deviations, of the critical nonlinear buckling loads are furnished by using Monte Carlo method and Quasi Monte Carlo simulation method. Finally, the applicability and the validity of the proposed approach are illustrated with a series of numerical investigations.

## Keywords

Generalized Chebyshev surrogate model; Hybrid random interval analysis; Time-dependent nonlinear buckling behaviour; 3D CFST; Structural stability

*,** Corresponding author: gaokang@seu.edu.cn; zhaoweig2002@163.com

## 1. **Introduction**

The design of structures to meet all kinds of criteria is always a crucial task for engineers. In static analysis, the arch-type structures will buckle in either an in-plane anti-symmetric bifurcation mode or in an in-plane symmetric snap-through mode with the constraint of lateral displacements and twist rotations, with corresponding critical buckling points named as bifurcation point and limit point. Such critical points are the boundary between the stability and instability of a structure, and when structures become unstable, it could fail catastrophically before reaching the serviceability limit state or yield strength of the materials. Therefore, in engineering design, it is critical to foresee the minimum buckling load of the structure so that the in-plane failure could be prevented[1, 2].

To date, many numerical researches on the buckling behaviour of arches have been extensively implemented[3-5]. The so-called classical buckling theory[6] has been applied to determine the critical buckling load of arches, however it may overestimate the buckling load of shallow arch[7]. This is because the classical buckling theory simplified the problem by linearizing the pre-buckling behaviour and ignoring the pre-buckling displacement[8]. An energy method is recently used by Pi [9, 10] in order to set up the non-linear equilibrium equations and buckling equilibrium equations for shallow arches with different cross-sections, loading and boundary conditions. Although these methods shown excellent performance on arch structures, the theories are derived based on 2D arches and in order to be applied to real engineering applications, complex 3D arch structures need to be simplified which could possibly lead to over or under estimation of the structural performance.

As one of the typical bridges, Concrete-filled steel tubular (CFST) arch bridges attracts large a number of attentions in both academic and industrial fields owing to their excellent mechanical behaviours and outstanding structural forms. Sun et al. [11] investigated the buckling behaviours of CFST arches subjected tilting loads via experimental study and verified by finite element analysis. By applying the machine learning method, Feng et al. [12] studied the stochastic effects of corrosion and fire on cables of CFST arches. Symmetric and asymmetric buckling of the arch structures were presented by Hu et al. [13]. Along with the development of the research, the time-dependent behaviours (such as creep and shrinkage effects) of CFST arches have been witnessed by many researches. Geng et al. [14-16] thoroughly studied the time-dependent behaviour of CFST arches and concluded that creep

effect induces remarkable effect on structural responses while shrinkage in the core concrete has little effect when the core concrete remains normal strength. Huang et al. [17] developed an analytical method for long-term lateral-torsional buckling behaviour of CFST arches subjected to uniform radial loads and temperature fields.

Besides the complexity of analysis procedures in stability design, intrinsic uncertainty and natural randomness are widely witnessed in the geometry and material characteristics. Such variations may change the equilibrium configuration and influence significantly the structural performance. As a result, the limit point and bifurcation point of the equilibrium path as well as the critical buckling load may change. Due to the manufacturing defects, the actual material/geometry may not match the exact design specifications, which will lead to the differences between experimental results and theoretical simulations. The inherent complexity in fabrication process, and inconsistent data measurement of experiments due to human errors will eventually lead to the uncertain structural responses [18, 19]. Until now, three main frameworks to handle the uncertainty have been broadly proposed, which are probabilistic/stochastic, non-probabilistic and hybrid approaches. As for the first type, uncertain variables are modelled as random parameters or random fields with specified distribution functions[20, 21]. While this approach needs large number of data to get the overall statistical information of structural outputs. The non-probabilistic approach[22, 23], addresses circumstances when stochastic demonstrating experiences challenges and lacks of sufficient statistical information. This approach includes fuzzy method [24, 25], interval analysis[26-28] and convex model with ellipsoidal uncertainties [29, 30] etc. In the hybrid approach, any combinations of the probabilistic and non-probabilistic analysis can be merged. Such method can obtain a more universal analysis framework by incorporating mixture of distinctive uncertainty models and gain a superior uncertainty analysis [31, 32].

To accurately assess the nonlinear critical buckling loads of a structure is a non-trivial task, and it gets even more challenging when uncertain parameters involved in the system. In engineering practices, the general finite element software has been extensive accepted by engineers for nonlinear buckling analysis with complex geometry. Although the rapid improvement of computational capability and the arise of efficiency algorithms, the computational cost of solving complex nonlinear structural problems is still too expensive. In this case, the direct sampling method does not applicable because obtaining the outputs are time-consuming but have no practical value. It has been recognized that alternative methods

can improve computational efficiency, such as importance sampling approach [33], subset simulation method [34] etc. These methods can significantly reduce the sampling size without sacrificing computational accuracy. Compared with traditional Monte Carlo simulation method, the sampling sizes are reduced but it is still inefficient uncertain systems with complex finite element models [28] or multiple types of random variables. Surrogate model or metamodel strategy [35-38] can obtain approximation expression between inputs (the area of interests) and outputs by using explicitly mathematical formulations. The benefit of this method is reflected in both sufficient accuracy and the time to find the statistical information can be drastically reduced.

In this paper, a new robust method is presented in assessing the time-dependent nonlinear buckling behaviour of CFST arch structures when both random and interval uncertainties are involved. The Chebyshev surrogate model strategy is adopted in formulating the relationships between the uncertain structural parameters and the critical nonlinear limit and bifurcation buckling loads based on finite element method. The QMCS and MCS methods are then combined to obtain the lower and upper bounds of the statistical characteristics of the critical nonlinear buckling loads. Both interval and random uncertain variables are considered in present framework.

This study is organized as follows. Section 2 introduces the general finite element procedure for buckling analysis with random and interval uncertainties are presented. In section 3, the generalized Chebyshev surrogate model-based sampling approach is presented. Section 4 introduces the time-dependent features of concrete. A series of numerical investigation are presented in section 5. Some conclusions are summarized in Section 6.

## 2. Stochastic interval nonlinear buckling analysis using finite element method

Assume $\zeta^R \in Z(\Re)$, and $Z(\Re)$ denotes overall random parameters in a stochastic set $(\mathbf{\Omega}, \mathbf{A}, \mathbf{P})$ and $\Re$ represents the set with all possible numbers. Also, $\xi^I = [\underline{\xi}, \overline{\xi}] \Leftrightarrow \{\xi \in \Re \,|\, \underline{\xi} \le \xi \le \overline{\xi}\}$ is an interval variable of $I(\Re)$ which denotes the set of all closed real intervals, where $\underline{\xi}$ and $\overline{\xi}$ denote respectively the lower and upper bounds of $\xi^I$.

For each time step $t + \Delta t$, applying the finite element method based on virtual work principle, one can obtain[39]:

$$ {}^{t+\Delta t}\mathbf{R} - {}^{t+\Delta t}\mathbf{F} = 0 \tag{1} $$

where ${}^{t+\Delta t}\mathbf{R}$ and ${}^{t+\Delta t}\mathbf{F}$ represent the vector of external forces and internal element stresses at time $t+\Delta t$, respectively. For static response of structures, the usual incremental solution of Eq.(1) can be presented as the following iterative scheme:

$$ {}^{\tau}\mathbf{K}^{(i-1)} \cdot \Delta\mathbf{U}^{(i)} = {}^{t+\Delta t}\mathbf{R} - {}^{t+\Delta t}\mathbf{F}^{(i-1)} \tag{2} $$

$$ {}^{t+\Delta t}\mathbf{U}^{(i)} = {}^{t+\Delta t}\mathbf{U}^{(i-1)} + \Delta\mathbf{U}^{(i)} \tag{3} $$

with the following initial conditions:

$$ {}^{t+\Delta t}\mathbf{F}^{(0)} = {}^{t}\mathbf{F};\ {}^{t+\Delta t}\mathbf{U}^{(0)} = {}^{t}\mathbf{U} \tag{4} $$

where ${}^{\tau}\mathbf{K}^{(i-1)}$ is a coefficient matrix and $\Delta\mathbf{U}^{(i)}$ is an increment displacement vector of the current one. It is also important to note that ${}^{\tau}\mathbf{K}^{(i-1)}$ is varying according to different iterations. In the full Newton-Raphson method, the matrix is updated in every iteration, i.e., ${}^{\tau}\mathbf{K}^{(i-1)} = {}^{t+\Delta t}\mathbf{K}^{(i-1)}$ and ${}^{t+\Delta t}\mathbf{K}^{(0)} = {}^{t}\mathbf{K}$ ; For modified Newton-Raphson iteration, the matrix updates at certain times, i.e., ${}^{\tau}\mathbf{K}^{(i-1)} = {}^{t}\mathbf{K}$ .

Such iterative method can only be applied to problems with prescribed load level for which the equilibrium configurations are to be calculated was known and only the response on the time of collapse of the structure was required. When the analyst does not have a pre-entry knowledge in structural loading capacity, and post-collapse response is required, the load-displacement-constraint method can be applied by introducing a load multiplier that increase or decrease the intensity of the externally applied loads [40-42]. In this case, Eq. (2) with modified Newton-Raphson iteration can be reformulated in the form:

$$ {}^{\tau}\mathbf{K} \cdot \Delta\mathbf{U}^{(i)} = {}^{t+\Delta t}\lambda\, \mathbf{R} - {}^{t+\Delta t}\mathbf{F}^{(i-1)} \tag{5} $$

where ${}^{t+\Delta t}\lambda$ is the load factor multiplier at time $t+\Delta t$ and $\mathbf{R}$ is the prescribed reference load vector. Based on deterministic iterative nonlinear finite element analysis framework, the non-deterministic analysis with uncertain parameters can be rewritten into:

$$ {}^{t}\mathbf{K}^{RI} \cdot \Delta\mathbf{U}^{RI\,(i)} = {}^{t+\Delta t}\lambda\, \mathbf{R}^{RI} - {}^{t+\Delta t}\mathbf{F}^{RI\,(i-1)} \tag{6} $$

where $(\bullet)^{RI}$ denotes the variable that is function of both random and interval uncertain parameters $\zeta^R$ and $\xi^I$, as follows

$$\begin{cases} \zeta^R \in \Omega := \{\zeta \in \Re^h \mid \zeta_d^R \sim g_{\zeta_d^R}(x), \quad \text{for } d = 1,...,h\} \\ \xi^I \in \mathbf{\Phi} := \{\xi \in \Re^v \mid \underline{\xi_c} \le \xi_c \le \overline{\xi_c}, \quad \text{for } c = 1,...,v\} \end{cases} \tag{7}$$

where $\zeta^R$ denotes the vector which collects all the $h$ random variables presented in the system; $g_{\zeta_d^R}(x)$ denotes the probability density function (PDF) of the random variable $\zeta_d^R$; $\mu_{\zeta_d^R}$ and $\sigma_{\zeta_d^R}$ represent the mean and standard deviation of random variable $\zeta_d^R$; $\xi^I$ is the interval variables presented in the system; $\underline{\xi_c}$ and $\overline{\xi_c}$ denote the lower and upper bounds of the $c$th interval variable. In most nonlinear buckling analysis methods for structures or engineering systems, this iterative method has been widely used in modern engineering applications for nonlinear buckling analysis. However, such method becomes difficult to implement when considering mixed uncertain parameters in the system.

## 3. The generalized Chebyshev surrogate model-based sampling approach

In this section, the proposed Chebyshev surrogate models are introduced to handle the random and/or interval uncertainty analysis. By transforming implicitly problem into an explicitly Chebyshev polynomials, such method can obtain highly acceptable accuracy. The classical sampling approach with MCS and/or QMCS method is then adopted so that the uncertain outputs of the critical nonlinear buckling loads can be obtained. For pure probabilistic analysis, the generalized Chebyshev surrogate model-based sampling approach is labelled as Chebyshev-MCS. In this category, the Chebyshev surrogate model is firstly generated, and after obtained the mathematical surrogated performance function the classical MCS is executed to capture the statistical features, such as means and standard deviations of the system outputs. In interval analysis, the proposed method is labelled as Chebyshev-QMCS, where QMCS is adopted after applying the Chebyshev surrogate model method and the upper and lower bounds of the interval outputs can be captured. This is because QMCS has superiority on generating more uniformly scattered random numbers which is particularly beneficial for modelling interval variables[43]. For the hybrid random interval analysis, again the Chebyshev surrogate model is firstly applied and the dual sampling approach which combines MCS and QMCS is adopted and termed as Chebyshev-MCS-QMCS method.

*3.1. Chebyshev polynomial*

According to the definition of Chebyshev polynomial, the domain $x \in [-1,1]$. For a more general domain $[a,b]$, it can be easily transferred to $[-1,1]$. The first kind of Chebyshev polynomial $T_n(x)$ with degree $n$ is defined as

$$T_n(x) = \cos[n \cdot \cos^{-1}(x)] \quad x \in [-1,1] \tag{8}$$

Substituting $n$=0,1 into Eq.(8), one can obtain

$$T_0(x) = 1,\ T_1(x) = \cos(\cos^{-1}(x)) = x \tag{9}$$

Furthermore, the following recurrence relation can generate

$$T_{n+1}(x) = 2xT_n(x) - T_{n-1}(x) \ \text{ when } \ n \geq 1 \tag{10}$$

Explicit expressions for the first 5 Chebyshev polynomials are:

$$T_0(x) = 1,\ T_1(x) = x,\ T_2(x) = 2x^2 - 1,\ T_3(x) = 4x^3 - 3x,\ T_4(x) = 8x^4 - 8x^2 + 1,\ \ldots \tag{11}$$

The polynomial $T_n(x)$ has $n$ zeros and $n$+1 extremum in the interval $[-1,1]$. The zeros of Chebyshev polynomial $T_n(x)$ are

$$x_j = \cos\frac{\pi(2j-1)}{2m} \quad j = 1,2,3,...,m \tag{12}$$

Chebyshev polynomial are orthogonal when $x \in [-1,1]$ with a weight function $w(x) = (1-x^2)^{-1/2}$, which has:

$$\int_{-1}^{1} T_i(x)T_z(x)w(x)\,\mathrm{d}x = N_i\delta_{iz} \tag{13}$$

with $N_0 = \pi$ and $N_i = \frac{\pi}{2}$ if $i \neq 0$, and $\delta_{iz}$ is Kronecher delta. In addition, the discrete orthogonal relationship is given as

$$\sum_{j=1}^{m} T_i(x_j)T_z(x_j) = K_i\delta_{iz} \tag{14}$$

with $K_0 = m$ and $K_i = \frac{m}{2}$ for $i \neq 0$.

For one dimensional problem, a target function $f(x)$ can be approximated in terms of Chebyshev series as:

$$f(x) \approx \sum_{i=0}^{n} a_i T_i(x) \tag{15}$$

where $n$ is the number of the Chebyshev series, and $a_i$ is the $i$-th coefficient of expansion. By multiplying equation $T_z(x_j)$ at both sides of Eq.(15) , one can obtain:

$$\sum_{j=1}^{m} f(x_j) T_z(x_j) = \sum_{i=0}^{n} a_i \left[\sum_{j=1}^{m} T_i(x_j) T_z(x_j)\right] = \sum_{i=0}^{n} a_i \, K_i \delta_{iz} \qquad i = 0,...z,...,n \tag{16}$$

where $m$=$n$+1 is the number of coefficients. The coefficient of expansion can then be expressed as:

$$\begin{cases} a_0 = \dfrac{1}{m} \displaystyle\sum_{j=1}^{m} f(x_j) \\ a_i = \dfrac{2}{m} \displaystyle\sum_{j=1}^{m} f(x_j) T_i(x_j), \quad i \geq 1 \end{cases} \tag{17}$$

For two-dimensional Chebyshev polynomials, $x_1$ and $x_2$ are considered, the following expression can be obtained

$$f(x_1, x_2) \approx \sum_{i_1=0}^{n_1} \sum_{i_2=0}^{n_2} a_{i_1 i_2} T_{i_1}(x_1) T_{i_2}(x_2) \tag{18}$$

Similarly, to find the coefficient $a_{i_1 i_2}$, Eq.(18) is expressed at zeros of $T_{n_1}(x)$ and $T_{n_2}(x)$, which are $x_1 = x_{j_1}$ and $x_2 = x_{j_2}$. Multiplying both sides of equation with $T_{z_1}(x_{j_1}) T_{z_2}(x_{j_2})$ and summing the resultant equations leads to:

$$\sum_{j_1=1}^{m_1} \sum_{j_2=1}^{m_2} f(x_{j_1}, x_{j_2}) T_{z_1}(x_{j_1}) T_{z_2}(x_{j_2}) = \sum_{i_1=0}^{n_1} \sum_{i_2=0}^{n_2} a_{i_1 i_2} \left[\sum_{j_1=0}^{m_1} T_{i_1}(x_{j_1}) T_{z_1}(x_{j_1})\right] \left[\sum_{j_2=0}^{m_2} T_{i_2}(x_{j_2}) T_{z_2}(x_{j_2})\right] \tag{19}$$

The coefficients for 2D model can be expressed by using Chebyshev orthogonality

$$\begin{cases} a_{00} = \dfrac{1}{m_1 m_2} \sum_{j_1=1}^{m_1} \sum_{j_2=1}^{m_2} f(x_{j_1}, x_{j_2}) \\ a_{i_1 0} = \dfrac{2}{m_1 m_2} \sum_{j_1=1}^{m_1} \sum_{j_2=1}^{m_2} f(x_{j_1}, x_{j_2}) T_{i_1}(x_{j_1}), \quad i_1 \geq 1 \\ a_{0 i_2} = \dfrac{2}{m_1 m_2} \sum_{j_1=1}^{m_1} \sum_{j_2=1}^{m_2} f(x_{j_1}, x_{j_2}) T_{i_2}(x_{j_2}), \quad i_2 \geq 1 \\ a_{i_1 i_2} = \dfrac{4}{m_1 m_2} \sum_{j_1=1}^{m_1} \sum_{j_2=1}^{m_2} f(x_{j_1}, x_{j_2}) T_{i_1}(x_{j_1}) T_{i_2}(x_{j_2}), \quad i_1 \geq 1, \quad i_2 \geq 1 \end{cases} \tag{20}$$

Following the same procedure, the Chebyshev polynomials of multi-dimensional system can be obtained by making the tensor product with respect to each one-dimensional polynomial, as follows

$$T_{n_1 \ldots n_k}(\mathbf{x}) = T_{n_1}(x_1) T_{n_2}(x_2) \ldots T_{n_k}(x_k), \ \mathbf{x} \in [-1, 1]^k \tag{21}$$

represents a *k*-dimensional Chebyshev polynomial. With regards to the orthogonality property, the multi-dimensional continuous function $f(\mathbf{x})$ can express as:

$$f(\mathbf{x}) \approx \sum_{i_1=0}^{n_1} \ldots \sum_{i_k=0}^{n_k} a_{i_1 \ldots i_k} T_{i_1 \ldots i_k}(\mathbf{x}) \tag{22}$$

where $n_k$ denotes the d.o.f Chebyshev polynomial in each dimension and the *k*-dimensional Chebyshev polynomials is rewritten as:

$$a_{i_1 \ldots i_k} = \left(\frac{1}{2}\right)^{\beta} \left(\frac{2^k}{m_1 m_2 \ldots m_k}\right) \sum_{j_1=1}^{m_1} \ldots \sum_{j_k=1}^{m_k} f(x_{j_1} \ldots x_{j_k}) T_{i_1 \ldots i_k}(x_{j_1} \ldots x_{j_k}) \tag{23}$$

where $\beta$ represents the occurrence of total number of zero(s) in the subscripts $i_1 \ldots i_k$, and $m_k = n_k + 1$.

## 4. The time-dependent features of concrete

In order to consider the time-dependent feature of concrete, the effective Young's modulus of the concrete is introduced [44, 45]:

$$E_{ec,t}(E_c, \phi_u, \phi_{\infty,7}, t) = \frac{1}{1 + \chi\ (t, \phi_{\infty,7}) \cdot \phi\ (t, \phi_u)} \cdot E_c \tag{24}$$

where $\phi\ (t,\phi_u)$ and $\chi\ (t,\phi_{\infty,7})$ are creep and aging coefficient, which are written as

$$\phi\ (t,\phi_u)=\left[\frac{(t-t_0)^{0.6}}{10+(t-t_0)^{0.6}}\right]\phi_u,\ \chi\ (t,\phi_{\infty,7})=1-\frac{(1-\chi^*(\phi_{\infty,7}))(t-t_0)}{20+(t-t_0)} \tag{25}$$

$\phi_{\infty,7}=0.8t_0^{0.118}\phi_u$ and

$$\chi^*(\phi_{\infty,7})=\frac{0.78t_0+0.4t_0e^{-1.33\phi_{\infty,7}}}{t_0+0.16+0.8e^{-1.33\phi_{\infty,7}}} \tag{26}$$

In this paper $t_0=15$ days is adopted to represent that first loading date of concrete.

## 5. Numerical Examples

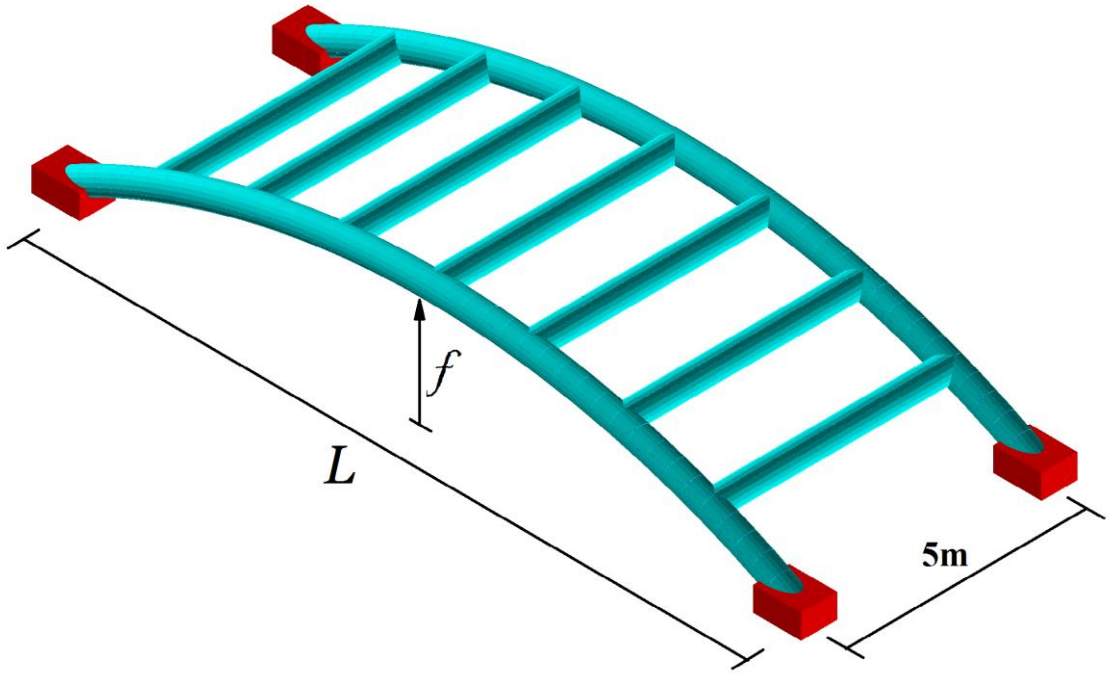


**Fig. 1.** 3D single span double CFST arch structure layout

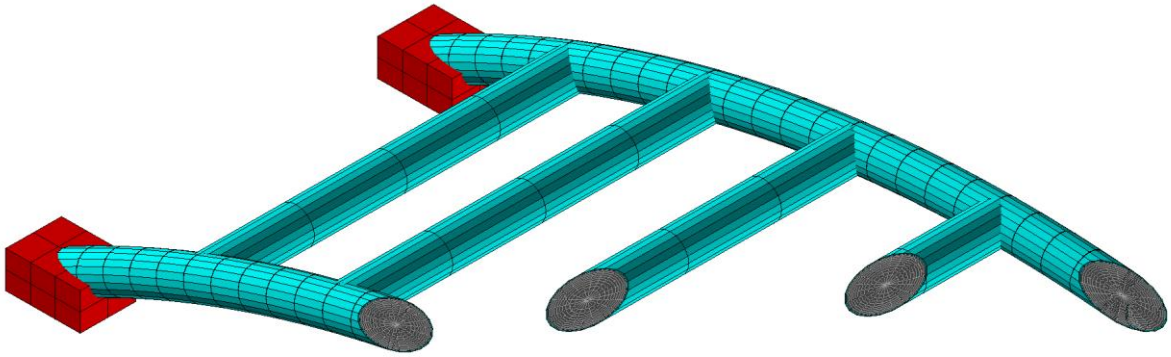

**Fig. 2.** Meshed 3D single span double CFST arch structure and internal section layout

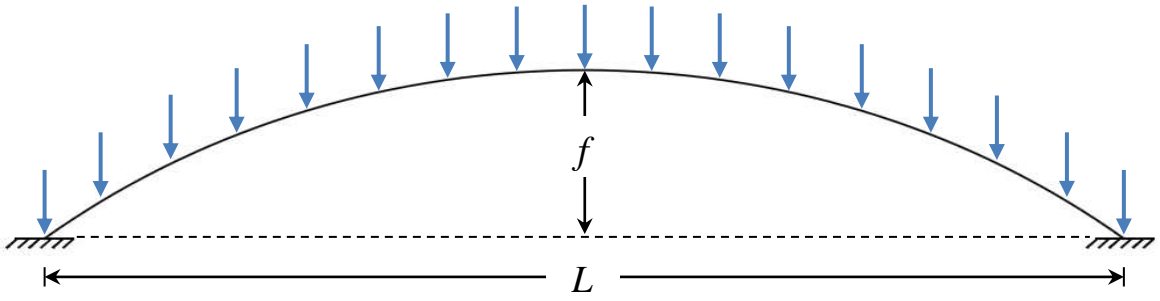


**Fig. 3.** Loading scenario on main arch span of CFST arch structure

In this section, the time-dependent uncertain random and/or interval bifurcation and limit point buckling load of 3D CFST arch structure is investigated to demonstrate the performance of the proposed generalized Chebyshev surrogate model-based sampling approach. The arch frame, shown in Fig. 1, is designed with a span $L = 15\,\text{m}$ and span-to-span width of 5m. The inner radius and outer radius of the main span and steel brace are $r_i = 0.24\,\text{m}$ and $r_o = 0.25\,\text{m}$, respectively. For the differences between bifurcation and limit point buckling, researchers have conducted many studies[46-48] and revealed that the type of buckling mode is influenced by geometrical properties and loading scenarios. In this study, all the loading scenarios are the same for both bifurcation buckling and limit point buckling analysis. Therefore, in the bifurcation buckling analysis, the rise-to-span ratio is designed to be 1/10.57 and in the limit point buckling analysis, it has a rise-to-span ratio of 1/12. The finite element simulations are implemented on ANSYS platform. For the 3D arch structure, the main span is linearized by 40 three-dimensional beam elements and each intermediate bracing is modelled by 4 three-dimensional beam elements, with a total of 594 degrees of freedom. The 2D arch structure is modelled separately as a single span structure linearized by 40 beam elements with a total of 234 degrees of freedom. Fig. 2 shows meshed structure and

section layout for the 3D arch. The applied vertical load is 600 kN on each node on the main arch span for both structures as indicated in Fig. 3.

Four possible uncertainty sources are considered. In the pure random scenario, the Young's modulus of steel and concrete are considered as normal distributed random variables with $\mu_{E_s^R} = 200$ GPa, $\sigma_{E_s^R} = 21$ GPa, $\mu_{E_c^R} = 30$ GPa and $\sigma_{E_c^R} = 3.6$ GPa; and in the pure interval scenario, the uncertain final creep coefficient is modelled as interval variable from 1.362 to 2.27 (i.e., $1.362 \le \phi_u^I \le 2.27$) and the final shrinkage coefficient is modelled as interval parameter which has $150\times10^{-6} \le \varepsilon_{sh}^{*I} \le 340\times10^{-6}$ [49-51]. In the hybrid random interval analysis, both random and interval uncertainty parameters are included.

For the pure random or interval analysis, the ANSYS Probabilistic Design System (PDS) is implemented as the reference method for verifying the random or interval bifurcation and limit point buckling analysis. In the ANSYS PDS, Monte Carlo simulation method was adopted for both probabilistic and interval analysis and was termed as ANSYS PDS-MCS. In the referenced hybrid random interval analysis, as ANSYS PDS does not provide direct double loop simulation function, ANSYS is thus run from MATLAB function for each uncertain simulation. In this approach, again the MCS and QMCS is adopted in generating samples from in MATLAB and the referenced method is termed as MATLAB-ANSYS-MCS-QMCS. For the QMCS approach, the low-discrepancy Sobol sequence is adopted by skipping the first 1000 values and retaining every 101$^{st}$ point for generating all the interval parameters.

In order to illustrate the difference between 2D and 3D structures, the bifurcation and limit point buckling analysis are carried at day 100 of the loading age at the mean and middle values of the uncertainty parameters. As shown in Fig. 4, both scenarios show a significant higher critical buckling load in 3D arch structures, which illustrates the necessity of implement 3D analysis and the deficiency of theoretical 2D study. The result why 3D model predicted a higher buckling load than the 2D model is that 3D models are prone to buckle out of the front plane and the steel braces of the 3D single span double CFST arch structure restraints this behaviour. Such conclusions have also been witnessed in columns, as reported by [52] and stated that *it was found that the theoretical buckling loads reported in previous*

*research with 2D systems were conservative and largely underestimated the buckling capacities of prestressed stayed columns.*

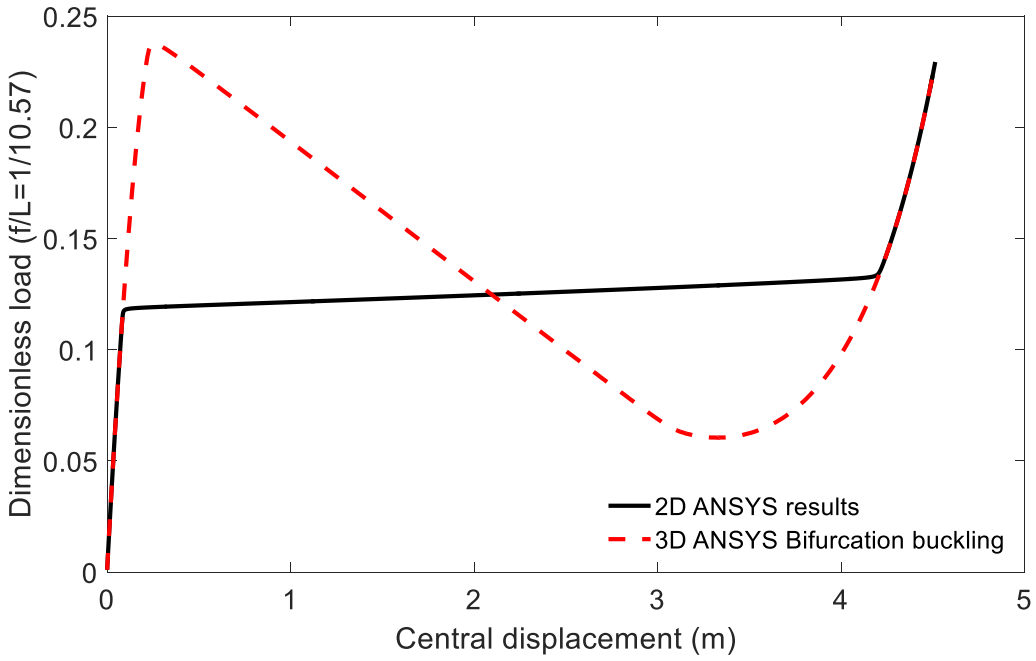


(a)

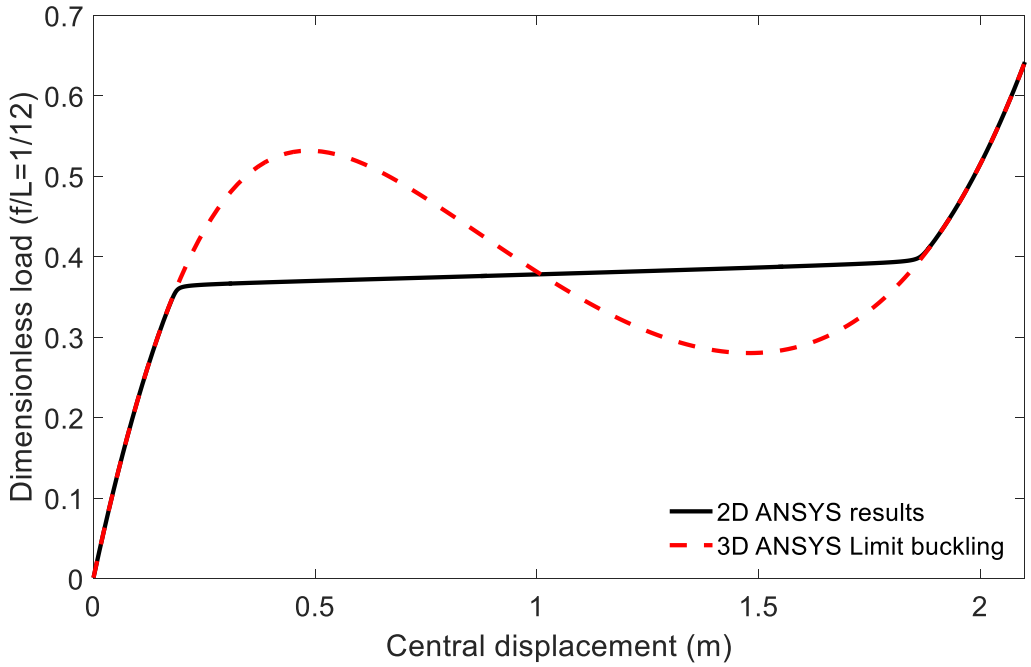


(b)

**Fig 4.** Critical buckling analysis of 2D and 3D CFST arch structures at day 100 for (a) bifurcation buckling and (b) limit point buckling

*5.1. Probabilistic analysis*

*5.1.1. Probabilistic bifurcation buckling of 3D CFST arch at day 100*

In the probabilistic analysis of bifurcation buckling of 3D CFST arch structure, the Young's modulus of concrete and steel are considered as random variables. For the proposed Chebyshev-MCS method, a mathematical function was first obtained by using Chebyshev polynomials where 14 interpolation points are selected in each dimension, and then 20000 MCS was performed to obtain the statistical information of the bifurcation point load and displacement. As the reference method, the ANSYS PDS-MCS method executed 5000 Monte Carlo simulations in ANSYS Probabilistic Design System (PDS), the mean and standard deviation of the relevant displacement and load at the bifurcation point was obtained. The relative error is calculated as:

$$\text{Relative error } (\%) = \frac{\text{Proposed method} - \text{Reference method}}{\text{Reference method}} \times 100$$

It can be seen in Table 1 that the ANSYS PDS-MCS took 9 hours and 20 minutes to finish the 5000 simulations, while the proposed method only took 30.7 minutes in generating the surrogate model and a flash of 30.5 seconds to finish the 20000 Monte Carlo simulations with an excellent accuracy.

**Table 1.** Bifurcation buckling analysis for pure random scenario

| Bifurcation buckling analysis | | | | |
|---|---|---|---|---|
| Pure random scenario | | | | |
| | μ of central displacement (m) | σ of central displacement (m) | μ of dimension-less load | σ of dimension-less load |
| Method 1 | 0.2571 | 0.0069 | 0.2379 | 0.0193 |
| Method 2 | 0.2571 | 0.0068 | 0.2375 | 0.0189 |
| Relative error (%) | 0.012 | -0.759 | -0.185 | -2.057 |
| | Method | Interpolation points | Simulation number | computational time |
| Method 1 | ANSYS PDS-MCS | N/A | 5000 | 9hrs 20mins |
| Method 2 | Chebyshev-MCS | 14*14 | 20000 | 30.7mins + 30.5s |

*5.1.2. Probabilistic limit point buckling of 3D CFST arch at day 100*

In the probabilistic analysis limit point buckling of 3D CFST arch structure, 8 interpolation points are selected in each dimension in order to formulate the surrogate model and again 20000 MCS was executed in the proposed Chebyshev-MCS approach and 5000 simulations in the ANSYS PDS-MCS method. It can be seen from Table 2 that again the proposed method achieved an excellent performance in both accuracy and efficiency.

**Table 2.** Limit point buckling analysis for pure random scenario

| Limit point buckling analysis | | | | |
|---|---|---|---|---|
| Pure random scenario | | | | |
| | μ of central displacement (m) | σ of central displacement (m) | μ of dimension-less load | σ of dimension-less load |
| Method 1 | 0.4856 | 0.0080 | 0.5321 | 0.0421 |
| Method 2 | 0.4867 | 0.0082 | 0.5314 | 0.0413 |
| Relative error (%) | 0.224 | 2.423 | -0.139 | -1.821 |
| | Method | Interpolation points | Simulation number | computational time |
| Method 1 | ANSYS PDS-MCS | N/A | 5000 | 15 hrs 13 mins |
| Method 2 | Chebyshev-MCS | 8*8 | 20000 | 22 mins + 37.8s |

*5.2. Interval analysis*

*5.2.1. Interval bifurcation buckling of 3D CFST arch at day 100*

In the interval analysis of bifurcation buckling of 3D CFST arch structure, the creep coefficient and final shrinkage coefficient are considered as interval variables. In the proposed Chebyshev-QMCS method, 3 interpolation points are selected in each interval dimension and 500 simulations were run based on the surrogated mathematical model. In the reference ANSYS PDS-MCS method, 1000 simulations have been implemented. The upper bound (U.B.) and lower bound (L.B.) of the central displacement and dimensionless load as well as the computational time and the relative errors are listed in Table 3. From Fig.5 it can be seen that the proposed Chebyshev-QMCS is capable of providing the load-displacement path before reaching the critical buckling load while for the ANSYS PDS-MCS only the critical loads can be captured with the indicated computational time. The buckling path calculated using the mid value of the interval inputs are also plot in Fig. 5.

**Table 3.** Bifurcation buckling analysis for pure interval scenario

| Bifurcation buckling analysis | | | | |
|---|---|---|---|---|
| Pure interval scenario | | | | |
| | U.B. of central displacement (m) | L.B. of central displacement (m) | U.B. of dimension-less load | L.B. of dimension-less load |
| Method 1 | 0.2618 | 0.2475 | 0.2469 | 0.2301 |
| Method 2 | 0.2609 | 0.2518 | 0.2468 | 0.2302 |
| Relative error (%) | -0.340 | 1.721 | -0.045 | 0.022 |
| | Method | Interpolation points | Simulation number | computational time |
| Method 1 | ANSYS PDS-MCS | N/A | 1000 | 1hrs 55mins |
| Method 2 | Chebyshev-QMCS | 3*3 | 500 | 1.7mins + 1.6s |

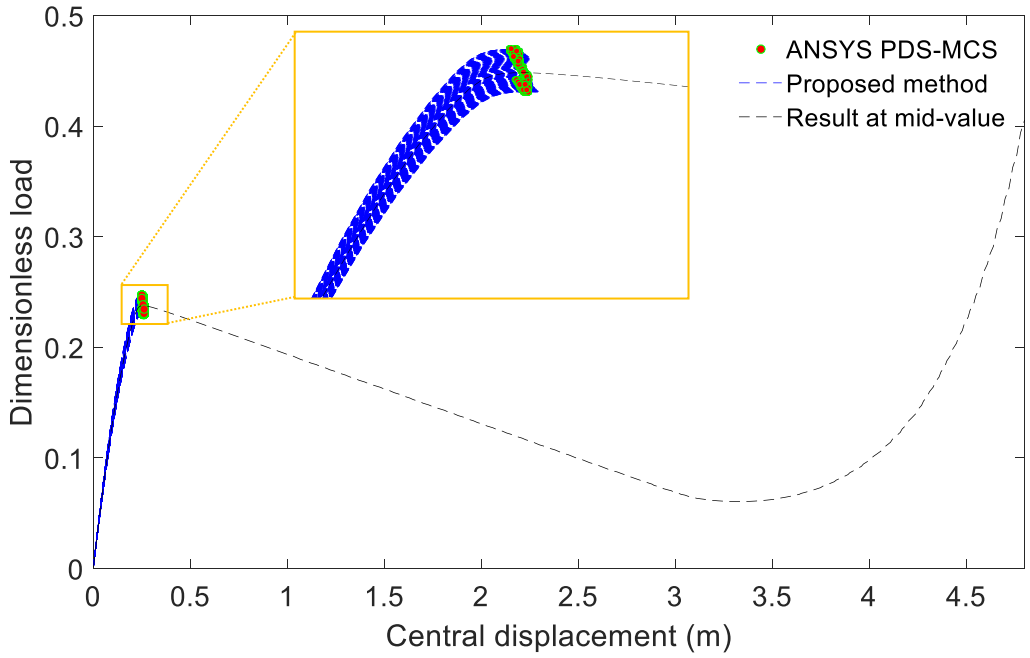


**Fig. 5.** Load displacement curve for bifurcation buckling analysis of 3D CFST arch with interval uncertainty parameters

*5.2.2. Interval limit point buckling of 3D CFST arch at day 100*

In the interval analysis of limit point buckling of 3D CFST arch structure, again 3 interpolation points are selected in each interval dimension and 500 simulations were run in Chebyshev-QMCS. 1000 simulations have been implemented in ANSYS PDS-MCS and the computational time and the relative errors are listed in Table 4. Fig. 6 shows the buckling path of each of the 500 interval inputs in the proposed Chebyshev-QMCS method, the critical

limit points captured using ANSYS PDS-MCS as well as the results from the mid values of the interval inputs.

**Table 4.** Limit point buckling analysis for pure interval scenario

| Limit point buckling analysis | | | | |
|---|---|---|---|---|
| Pure interval scenario | | | | |
| | U.B. of central displacement (m) | L.B. of central displacement (m) | U.B. of dimension-less load | L.B. of dimension-less load |
| Method 1 | 0.4958 | 0.4733 | 0.5566 | 0.5117 |
| Method 2 | 0.4917 | 0.4709 | 0.5562 | 0.5118 |
| Relative error (%) | -0.835 | -0.513 | -0.070 | 0.029 |
| | Method | Interpolation points | Simulation number | computational time |
| Method 1 | ANSYS PDS-MCS | N/A | 1000 | 3 hrs 10 mins |
| Method 2 | Chebyshev-QMCS | 3*3 | 500 | 2.3mins +2.4s |

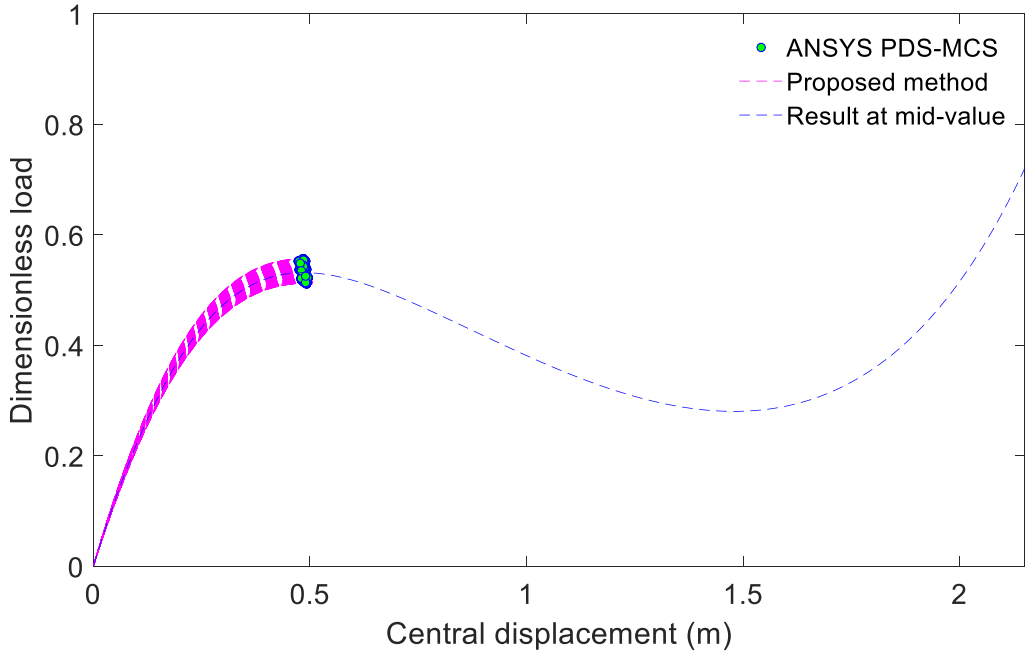


**Fig.6.** Load displacement curve for limit point buckling analysis of 3D CFST arch with interval uncertainty parameters

*5.3. Hybrid random interval analysis*

5.3.1. *Results verification for hybrid analysis at day 100*

In this section, the varication for hybrid random interval bifurcation buckling analysis of 3D CFST arch structures at day 100 of the loading age was firstly implemented. As aforementioned, both uncertain variables in pure probabilistic and interval analysis are incorporated in the hybrid analysis. In the proposed Chebyshev-MCS-QMCS method, 14 interpolation points are selected in each dimension for random variables and 3 interpolation points are selected in each dimension for interval variables. The Chebyshev polynomials are then constructed followed by a combination of 1000 MCS and 500 QMCS. In the reference method, however, the combination of 1000 MCS and 500 QMCS are run in ANSYS from MATLAB function. It has been noticed that the reference method took a huge amount of computational time, in which 20 computers were involved and it took 76 hours 10 minutes for each computer to finish the simulation. While in the proposed Chebyshev-MCS-QMCS method, it consumed 4.35 hours to generate the Chebyshev surrogate model, and after that only 48 minutes was used to finish the 500,000 simulations. The relative errors which show the exceptional computational accuracy achieved by the proposed method are also listed in Table 5.

**Table 5.** Bifurcation buckling analysis at day 100 for hybrid random interval scenario

| Bifurcation buckling analysis at Day 100 | | | | |
|---|---|---|---|---|
| Hybrid random interval scenario | | | | |
| | U.B. of μ of central displacement (m) | L.B. of μ of central displacement (m) | U.B. of σ of central displacement (m) | L.B. of σ of central displacement (m) |
| Method 1 | 0.2558 | 0.241 | 0.0081 | 0.0068 |
| Method 2 | 0.2564 | 0.2395 | 0.0084 | 0.0066 |
| Relative error (%) | 0.2346 | -0.6224 | 3.7037 | -2.9412 |
| | U.B. of μ of dimensionless load | L.B. of μ of dimensionless load | U.B. of σ of dimensionless load | L.B. of σ of dimensionless load |
| Method 1 | 0.2463 | 0.2301 | 0.0201 | 0.0177 |
| Method 2 | 0.2477 | 0.2293 | 0.0201 | 0.0175 |
| Relative error (%) | 0.568 | -0.348 | 0.178 | -1.130 |
| | Method | Interpolation | Simulation | computational |

| | | points | number | time |
|---|---|---|---|---|
| Method 1 | MATLAB-ANSYS –MCS-QMCS | N/A | 1000*500 | 20*76 hr 10mins |
| Method 2 | Chebyshev-MCS-QMCS | 14*14*3*3 | 1000*500 | 4.35 hr + 48mins |

*5.3.2. Hybrid random interval bifurcation buckling of 3D CFST arch*

After the varication stage, the hybrid random interval bifurcation buckling analysis of 3D CFST arch structures has been further implemented at day 50 and day 400 of the loading age. The detailed results and computational time are listed in Table 6 and Table 7. The upper and lower bounds of the mean of the loading path as well as the results calculated using the mean and mid values of the input uncertainty variables are plot in Fig. 7. Due to the exceptional computation efforts required in performing the MATLAB-ANSYS–MCS-QMCS analysis, the results verification for day 50 and day 400 of the hybrid random interval bifurcation buckling analysis is not taken place.

**Table 6.** Bifurcation buckling analysis at day 50 and 400 for hybrid random interval scenario

| Bifurcation buckling analysis | | | | |
|---|---|---|---|---|
| Hybrid random interval scenario | | | | |
| | U.B. of μ of central displacement (m) | L.B. of μ of central displacement (m) | U.B. of σ of central displacement (m) | L.B. of σ of central displacement (m) |
| Day 50 | 0.2572 | 0.2481 | 0.0072 | 0.0059 |
| Day 400 | 0.2671 | 0.256 | 0.0106 | 0.0056 |
| | U.B. of μ of dimensionless load | L.B. of μ of dimensionless load | U.B. of σ of dimensionless load | L.B. of σ of dimensionless load |
| Day 50 | 0.2553 | 0.2361 | 0.0209 | 0.0181 |
| Day 400 | 0.2391 | 0.2208 | 0.0197 | 0.0171 |
| | Method | Interpolation points | Simulation number | |
| | Chebyshev-MCS-QMCS | 14*14*3*3 | 1000*500 | |

**Table 7.** Computational time for Bifurcation buckling analysis with Hybrid scenario

| Computational time for Bifurcation buckling analysis with Hybrid scenario | |
|---|---|
| Day 50 | Day 400 |
| 5.20hrs + 41.12mins | 4.81hrs+ 45.96mins |

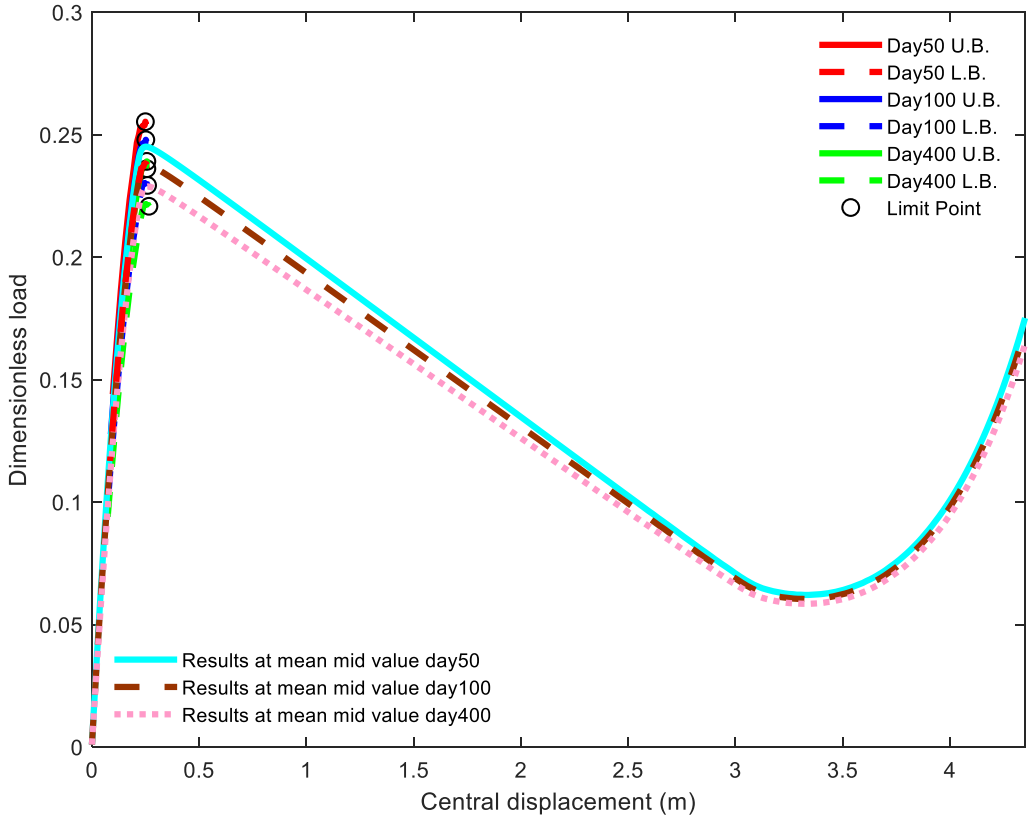


**Fig.7.** The upper and lower bounds of the mean of the load displacement curve for bifurcation buckling analysis of 3D CFST arch with hybrid random interval uncertainty parameters

*5.3.3. Hybrid random interval limit point buckling of 3D CFST arch*

The limit point buckling analysis of 3D CFST arch at day 50, 100 and 400 of the loading ages with both random and interval variables are implemented in this section. In the proposed Chebyshev-MCS-QMCS method, 8 interpolation points are selected in each dimension for random variables and 3 interpolation points are selected in each dimension for interval variables. The results and computational time are listed in Table 8 and Table 9, and the upper and lower bounds of the mean of the loading path as well as the results calculated using the mean and mid values of the input uncertainty variables are plot in Fig. 8. Again, due to the exceptional computation efforts required in performing the reference method, the results have not been verified. The purpose of section 4.3.2 and 4.3.3 is major showing the potential and capability of the proposed Chebyshev-MCS-QMCS method in performing time-

dependent hybrid probabilistic interval non-linear buckling analysis. It has also been noticed that with the increase of loading age, the upper and lower bounds of the mean of the critical bifurcation of limit point buckling load will decrease. The proposed method can efficiently and accurately foresee such change at the design stage when both random and interval uncertainty factors are involved.

**Table 8.** Limit point buckling analysis for hybrid random interval scenario

| Limit point buckling analysis | | | | |
|---|---|---|---|---|
| Hybrid random interval scenario | | | | |
| | U.B. of μ of central displacement (m) | L.B. of μ of central displacement (m) | U.B. of σ of central displacement (m) | L.B. of σ of central displacement (m) |
| Day 50 | 0.4868 | 0.4743 | 0.0094 | 0.0059 |
| Day 100 | 0.4911 | 0.4791 | 0.0099 | 0.0069 |
| Day 400 | 0.4971 | 0.4833 | 0.0095 | 0.0062 |
| | U.B. of μ of dimensionless load | L.B. of μ of dimensionless load | U.B. of σ of dimensionless load | L.B. of σ of dimensionless load |
| Day 50 | 0.5763 | 0.5301 | 0.0466 | 0.0390 |
| Day 100 | 0.5578 | 0.5111 | 0.0454 | 0.0384 |
| Day 400 | 0.5344 | 0.4883 | 0.0426 | 0.0372 |
| | Method | Interpolation points | Simulation number | |
| | Chebyshev-MCS-QMCS | 8*8*3*3 | 1000*500 | |

**Table 9.** Computational time for limit point buckling analysis with Hybrid scenario

| Computational time for limit point buckling analysis with Hybrid scenario | | |
|---|---|---|
| Day 50 | Day 100 | Day 400 |
| 2.56hrs + 72.72mins | 2.51hrs + 73.03mins | 2.45hrs + 70.40 mins |

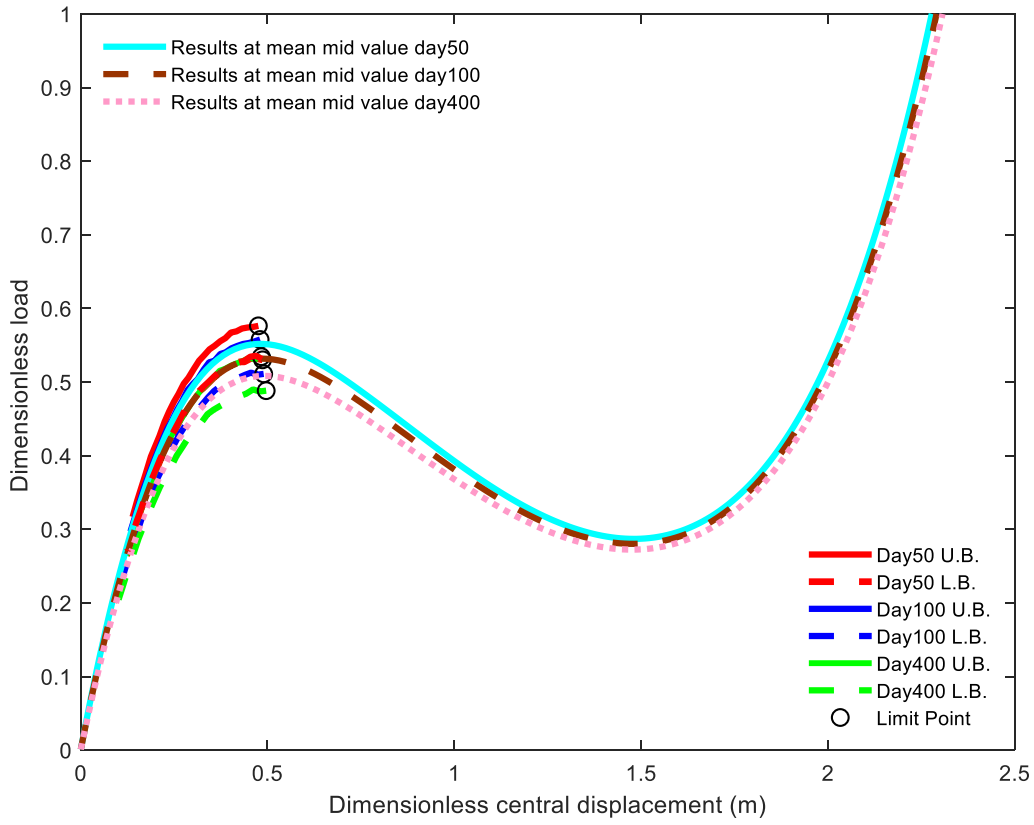


**Fig.8.** The upper and lower bounds of the mean of the load displacement curve for limit point buckling analysis of 3D CFST arch with hybrid random interval uncertainty parameters

## 6. Conclusions

This study has proposed a new generalized Chebyshev surrogate model based on sampling approach in analysing the time-dependent nonlinear buckling behaviour of CFST arch structures when both probabilistic and interval uncertainties are incorporated. With the Chebyshev surrogate model strategy combined with finite element method, the mathematical relationships between the uncertain structural parameters and the critical nonlinear limit and bifurcation buckling loads can be formulated explicitly, which dramatically reduced the computational time when performing uncertainty analysis using MCS and QMCS methods. With the exceptional computational efficiency, the proposed method can be used to perform nonlinear buckling analysis of CFST arch structures at any time of the loading age and accurately predict the critical buckling loads and load-displacement paths. Furthermore, with the help of finite element method, the proposed approach is capable of analysing nonlinear buckling of complex 3D structures with hybrid random interval uncertainties.

## Acknowledgements

The work described in the present paper is fully funded by a research grant from the National Natural Science Foundation of China (51838004), the National Key Research and Development Program of China (2020YFC1511900), Natural Science Foundation of Jiangsu Province (BK20210254), 2021 High-level Personnel Project Funding of Jiangsu Province (JSSCBS20210069) as well as the funding from State Key Laboratory of Mechanical Behavior and System Safety of Traffic Engineering Structures (KF2022-04). The authors are grateful for the financial support. The damage dataset supporting the conclusions of this article will be made available by the authors, without reservation.

## Declaration of Interests

All authors declare that they do not have any conflict of interest in the work presented in this paper.

## Reference


[1] Dou C, Guo Y-F, Jiang Z-Q, Gao W, Pi Y-L. In-plane buckling and design of steel tubular truss arches. Thin-Walled Structures. 2018;130:613-21.

[2] Dou C, Jiang Z-Q, Pi Y-L, Gao W. Elastic buckling of steel arches with discrete lateral braces. Engineering Structures. 2018;156:12-20.

[3] Liu A-R, Huang Y-H, Fu J-Y, Yu Q-C, Rao R. Experimental research on stable ultimate bearing capacity of leaning-type arch rib systems. Journal of Constructional Steel Research. 2015;114:281-92.

[4] Liu A, Lu H, Fu J, Pi Y-L, Huang Y, Li J et al. Analytical and experimental studies on out-of-plane dynamic instability of shallow circular arch based on parametric resonance. Nonlinear Dynamics. 2017;87:677-94.

[5] Liu A, Yang Z, Bradford MA, Pi Y-L. Nonlinear Dynamic Buckling of Fixed Shallow Arches under an Arbitrary Step Radial Point Load. Journal of Engineering Mechanics. 2018;144:04018012.

[6] Timoshenko SP, Gere JM. Theory of elastic stability. McGraw-Hill, New York; 1961.

[7] Pi Y-L, Bradford M, Uy B. In-plane stability of arches. Int J Solids Struct. 2002;39:105-25.

[8] Pi Y-L, Trahair N. Non-linear buckling and postbuckling of elastic arches. Engineering Structures. 1998;20:571-9.

[9] Pi Y-L, Bradford M, Tin-Loi F. Nonlinear analysis and buckling of elastically supported circular shallow arches. Int J Solids Struct. 2007;44:2401-25.

[10] Pi Y-L, Bradford MA, Qu W. Long-term non-linear behaviour and buckling of shallow concrete-filled steel tubular arches. Int J Nonlinear Mech. 2011;46:1155-66.

[11] Sun J, Geng Y, Zhang H, Yin H, Wang Y. Experimental and numerical study on slender concrete-filled steel tubular arches subjected to tilting loads. Thin-Walled Structures. 2022;179:109701.

[12] Feng J, Gao K, Gao W, Liao Y, Wu G. Machine learning-based bridge cable damage detection under stochastic effects of corrosion and fire. Engineering Structures. 2022;264:114421.

[13] Hu C-F, Li Z, Hu Q-S. On non-linear behavior and buckling of arch-beam structures. Engineering Structures. 2021;239:112214.

[14] Geng Y, Ranzi G, Wang Y, Zhang S. Time-dependent behaviour of concrete-filled steel tubular columns: analytical and comparative study. Magazine of Concrete Research. 2012;64:55-69.

[15] Geng Y, Ranzi G, Wang Y-T, Wang Y-Y. Out-of-plane creep buckling analysis on slender concrete-filled steel tubular arches. Journal of Constructional Steel Research. 2018;140:174-90.

[16] Geng Y, Wang Y, Ranzi G, Wu X. Time-dependent analysis of long-span, concrete-filled steel tubular arch bridges. Journal of Bridge Engineering. 2014;19:04013019.

[17] Huang Y, Yang Z, Fu J, Liu A. Long-term lateral-torsional buckling behavior of pin-ended CFST arches under uniform radial loads and temperature field. Mechanics of Advanced Materials and Structures. 2021;28:2472-86.

[18] Ellingwood BR, Tekie PB. Wind load statistics for probability-based structural design. Journal of Structural Engineering. 1999;125:453-63.

[19] Gao W, Song C, Tin-Loi F. Probabilistic interval analysis for structures with uncertainty. Structural Safety. 2010;32:191-9.

[20] Barbato M, Zona A, Conte JP. Probabilistic nonlinear response analysis of steel-concrete composite beams. Journal of Structural Engineering. 2013;140:04013034.

[21] Ma J, Zhang S, Wriggers P, Gao W, De Lorenzis L. Stochastic homogenized effective properties of three-dimensional composite material with full randomness and correlation in the microstructure. Computers & Structures. 2014;144:62-74.
[22] Moens D, Vandepitte D. A survey of non-probabilistic uncertainty treatment in finite element analysis. Computer methods in applied mechanics and engineering. 2005;194:1527-55.
[23] Möller B, Beer M. Engineering computation under uncertainty–capabilities of non-traditional models. Comput Struct. 2008;86:1024-41.
[24] Brown CB, Yao JT. Fuzzy sets and structural engineering. Journal of structural engineering. 1983;109:1211-25.
[25] Wang L, Ma Y, Zhang J, Liu Y. Probabilistic analysis of corrosion of reinforcement in RC bridges considering fuzziness and randomness. Journal of Structural Engineering. 2012;139:1529-40.
[26] Do DM, Gao W, Song C, Tangaramvong S. Dynamic analysis and reliability assessment of structures with uncertain-but-bounded parameters under stochastic process excitations. Reliability Engineering & System Safety. 2014;132:46-59.
[27] Yang C, Tangaramvong S, Tin-Loi F, Gao W. Influence of interval uncertainty on the behavior of geometrically nonlinear elastoplastic structures. Journal of Structural Engineering. 2016;143:04016147.
[28] Gao K, Gao W, Wu B, Song C. Nondeterministic dynamic stability assessment of Euler–Bernoulli beams using Chebyshev surrogate model. Applied Mathematical Modelling. 2019;66:1-25.
[29] Kang Z, Luo Y. Non-probabilistic reliability-based topology optimization of geometrically nonlinear structures using convex models. Computer Methods in Applied Mechanics and Engineering. 2009;198:3228-38.
[30] Jiang C, Han X, Lu G, Liu J, Zhang Z, Bai Y. Correlation analysis of non-probabilistic convex model and corresponding structural reliability technique. Computer Methods in Applied Mechanics and Engineering. 2011;200:2528-46.
[31] Wu J, Luo Z, Zhang N, Zhang Y. A new uncertain analysis method and its application in vehicle dynamics. Mechanical Systems and Signal Processing. 2015;50:659-75.
[32] Wu B, Gao W, Wu D, Song C. Probabilistic interval geometrically nonlinear analysis for structures. Structural Safety. 2017;65:100-12.
[33] Au S, Beck J. Important sampling in high dimensions. Structural safety. 2003;25:139-63.
[34] Elishakoff I, Dujat K, Lemaire M, Gadiot G. Hybrid Optimization and Anti-Optimization of a Stochastically Excited Beam. Journal of Applied Mechanics. 2014;81:021017.
[35] Yao TH-J, Wen Y-K. Response surface method for time-variant reliability analysis. Journal of Structural Engineering. 1996;122:193-201.
[36] Bakalis K, Fragiadakis M, Vamvatsikos D. Surrogate modeling for the seismic performance assessment of liquid storage tanks. Journal of Structural Engineering. 2016;143:04016199.
[37] Wu J, Luo Z, Zhang N, Gao W. A new sequential sampling method for constructing the high-order polynomial surrogate models. Engineering Computations. 2018;35:529-64.
[38] Wu J, Luo Z, Zheng J, Jiang C. Incremental modeling of a new high-order polynomial surrogate model. Applied Mathematical Modelling. 2016;40:4681-99.
[39] Bathe K-J. Finite element procedures in engineering analysis. Prentice-Hall; 1982.
[40] Riks E. An incremental approach to the solution of snapping and buckling problems. Int J Solids Struct. 1979;15:529-51.

[41] Bathe K-J, Dvorkin EN. On the automatic solution of nonlinear finite element equations. Nonlinear Finite Element Analysis and Adina: Elsevier; 1983. p. 871-9.
[42] Bathe K-J. Finite element procedures: Klaus-Jurgen Bathe; 2006.
[43] Zhang H, Dai H, Beer M, Wang W. Structural reliability analysis on the basis of small samples: an interval quasi-Monte Carlo method. Mechanical Systems and Signal Processing. 2013;37:137-51.
[44] Australia SAo. AS3600. Australian Standard: Concrete Structures. Sydney2001.
[45] Institute AC. ACI Committee 209. Prediction of creep, shrinkage and temperature effects in concrete structures. Detroit1982.
[46] Chen C-N. A finite element study on bifurcation and limit point buckling of elastic-plastic arches. Computers & structures. 1996;60:189-96.
[47] Samuels P. Bifurcation and limit point instability of dual eigenvalue third order systems. Int J Solids Struct. 1980;16:743-56.
[48] Wardle BL, Lagace PA. Bifurcation, limit-point buckling, and dynamic collapse of transversely loaded composite shells. AIAA journal. 2000;38:507-16.
[49] Ichinose LH, Watanabe E, Nakai H. An experimental study on creep of concrete filled steel pipes. Journal of constructional steel research. 2001;57:453-66.
[50] Uy B. Static long-term effects in short concrete-filled steel box columns under sustained loading. Structural Journal. 2001;98:96-104.
[51] Han L-H, Tao Z, Liu W. Effects of sustained load on concrete-filled hollow structural steel columns. Journal of structural engineering. 2004;130:1392-404.
[52] Hyman P, Osofero AI, Sriramula S. Buckling behaviour of three-dimensional prestressed stayed columns. IOP Conference Series: Materials Science and Engineering: IOP Publishing; 2018. p. 012007.